THE JOURNAL OF BIOLOGICAL CHEMISTRY VOL. 284, NO. 33, pp. 22274–22284, August 14, 2009


# Functional Cross-talk between β-Catenin and NFκB Signaling Pathways in Colonic Crypts of Mice in Response to Progastrin*

Received for publication, May 14, 2009 Published, JBC Papers in Press, June 4, 2009, DOI 10.1074/jbc.M109.020941

**Shahid Umar**[‡§1], **Shubhashish Sarkar**[¶1], **Yu Wang**[¶], **and Pomila Singh**[¶2]

*From the* [‡]*Department of Internal Medicine, University of Oklahoma Health Sciences Center, Oklahoma City, Oklahoma 73104 and the Departments of* [¶]*Neuroscience and Cell Biology and* [§]*Internal Medicine, University of Texas Medical Branch, Galveston, Texas 77555*

**We recently reported a critical role of NFκB in mediating hyperproliferative and anti-apoptotic effects of progastrin on proximal colonic crypts of transgenic mice overexpressing progastrin (Fabp-PG mice). We now report activation of β-catenin in colonic crypts of mice in response to chronic (Fabp-PG mice) and acute (wild type FVB/N mice) progastrin stimulation. Significant increases were measured in relative levels of cellular and nuclear β-catenin and pβ-cat$^{45}$ in proximal colonic crypts of Fabp-PG mice compared with that in wild type littermates. Distal colonic crypts were less responsive. Interestingly, β-catenin activation was downstream of IKKα,β/NFκB, because treatment of Fabp-PG mice with the NFκB essential modulator (NEMO) peptide (inhibitor of IKKα,β/NFκB activation) significantly blocked increases in cellular/nuclear levels of total β-catenin/pβ-cat$^{45}$/and pβ-cat$^{552}$ in proximal colons. Cellular levels of pβ-cat$^{33,37,41}$, however, increased in proximal colons in response to NEMO, probably because of a significant increase in pGSK-3β$^{Tyr216}$, facilitating degradation of β-catenin. NEMO peptide significantly blocked increases in cyclin D1 expression, thereby, abrogating hyperplasia of proximal crypts. Goblet cell hyperplasia in colonic crypts of Fabp-PG mice was abrogated by NEMO treatment, suggesting a cross-talk between the NFκB/β-catenin and Notch pathways. Cellular proliferation and crypt lengths increased significantly in proximal but not distal crypts of FVB/N mice injected with 1 nM progastrin associated with a significant increase in cellular/nuclear levels of total β-catenin and cyclin D1. Thus, intracellular signals, activated in response to acute and chronic stimulation with progastrin, were similar and specific to proximal colons. Our studies suggest a novel possibility that activation of β-catenin, downstream to the IKKα,β/NFκB pathway, may be integral to the hyperproliferative effects of progastrin on proximal colonic crypts.**

Accumulating evidence suggests that gastrins play an important role in proliferation and carcinogenesis of gastrointestinal and pancreatic cancers (1, 2). Progastrin and glycine-extended gastrin (G-Gly)[3] are predominant forms of gastrins found in many tumors, including colon (3–5). Progastrin exerts potent proliferative and anti-apoptotic effects *in vitro* and *in vivo* on intestinal mucosal cells (6–10) and on pancreatic cancer cells (11). Transgenic mice overexpressing progastrin from either the liver (hGAS) or intestinal epithelial cells (Fabp-PG) are at a higher risk for developing pre-neoplastic and neoplastic lesions in colons in response to azoxymethane (12–15). Treatment with G-Gly similarly increased the risk for developing pre-neoplastic lesions in rats (16). Thus progastrin and G-Gly exert co-carcinogenic effects *in vivo* (12–16).

Under physiological conditions, only processed forms of gastrins (G17, G34) are present in the circulation (17). In certain disease states, elevated levels of circulating progastrin (0.1 to >1.0 nM) are measured (1). Because co-carcinogenic effects of progastrin are measured in Fabp-PG mice, which express pathophysiological concentrations of hProgastrin (<1–5 nM) (12), elevated levels of circulating progastrin measured in certain disease states in humans may play a role in colon carcinogenesis. A curious finding was that pre-neoplastic and neoplastic lesions were significantly increased in proximal, but not distal, colons of Fabp-PG mice, in response to azoxymethane (12, 14), which may reflect an increase in proliferation and a decrease in azoxymethane-induced apoptosis in proximal colons of Fabp-PG mice (18). We reported a critical role of NFκB activation in mediating proliferation and the anti-apoptotic effect of progastrin on pancreatic cancer cells (*in vitro*) and on proximal colonic crypts of Fabp-PG mice (*in vivo*) (11, 18). Whereas the Wnt/β-catenin pathway is known to play a role in the proliferation of colonic crypts (19), its role in mediating biological effects of progastrin remains unknown.

β-Catenin is regulated by canonical (GSK-3β phosphorylation-dependent) and non-canonical (GSK-3β phosphorylation-independent) pathways. In the canonical pathway, inhibition of GSK-3β protects β-catenin against degradation by protein complexes, consisting of GSK-3β, axin, and adenomatous polyposis coli (20). In a resting cell, β-catenin is not present in the cytoplasm or nucleus because of proteasomal degradation of β-catenin that is not bound to E-cadherin (20).

* This work was supported, in whole or in part, by National Institutes of Health Grants R01 CA97959 and CA114264 (to P. S.) and R01 CA131413 (to S. U.) from the NCI.

[1] Both authors contributed equally to this work.

[2] To whom correspondence should be addressed: Dept. of Neuroscience and Cell Biology, 10.104 Medical Research Bldg., Route 1043, University of Texas Medical Branch, Galveston, TX 77555-1043. Tel.: 409-772-4842; Fax: 409-772-3222; E-mail: posingh@utmb.edu.

[3] The abbreviations used are: G-Gly, glycine-extended gastrin; ERK, extracellular signal-regulated kinase; Fabp, fatty acid-binding protein promoter; GSK-3β, glycogen synthase kinase-3β; IKK, IκBα kinase; NFκB, nuclear factor κB; NEMO, NFκB essential modulator; PCNA, proliferating cell nuclear antigen; PG, progastrin; WT, wild type; IHC, immunohistochemistry.

Following inactivation of GSK-3β, β-catenin stabilizes in the cytoplasm and translocates to the nucleus where it cooperates with Tcf/Lef for activation of target genes (20). In the current studies, we examined whether β-catenin is activated in proximal *versus* distal colonic crypts of Fabp-PG mice. Relative levels of β-catenin and its target gene product, cyclin D1, were significantly increased in proximal *versus* distal colonic crypts of Fabp-PG mice. We next examined a possible cross-talk between NFκB and β-catenin activation and the role of GSK-3β. Our results suggest the novel possibility that β-catenin activation in response to progastrin is downstream to IKKα,β/NFκB p65 activation, and that phosphorylation of GSK-3β at $Tyr^{216}$ may be critically involved.

To examine whether differences measured in the response of proximal *versus* distal colons in Fabp-PG mice were not an artifact of chronic stimulation, we additionally injected WT FVB/N mice with progastrin, as an acute model of stimulation. Our results confirmed that differences we had measured in Fabp-PG mice are not an artifact of chronic stimulation but represent inherent differences in the response of proximal *versus* distal colonic crypts to circulating progastrins.

We and others (18, 21) have previously demonstrated goblet cell hyperplasia in colonic crypts of transgenic mice overexpressing progastrin. In the current studies, we confirmed a significant increase in goblet cell hyperplasia/metaplasia (?) in proximal colonic crypts of Fabp-PG mice. Importantly, goblet cell hyperplasia was reversed to wild type levels by attenuating NFκB activation (and hence β-catenin activation) in NEMO-treated mice. The results of the current studies thus further suggest that pathways which dictate goblet cell lineage may be modulated by progastrin and may be downstream of NFκB/β-catenin activation. This represents a novel paradigm, which needs to be further examined.

## EXPERIMENTAL PROCEDURES

*Housing of Fabp-PG Mice*—Fabp-PG mice were generated by our laboratory as described (12). The fatty acid-binding protein (Fabp) promoter was used to drive the expression of human gastrin cDNA in the small and large intestines. The Fabp-PG transgenic mice and their WT littermates were bred and housed in the animal housing facility at UTMB, using protocols approved by the Institutional Animal Care and Use Committee (IACUC) at UTMB. Mice were housed in a microisolator, solid-bottomed, polycarbonate cages, and were maintained on a commercial diet (M/R Rodent Sterile Diet 7012; Harlan Tech Labs, Indianapolis, IN) with autoclaved water available *ad libitum*. Age-matched female Fabp-PG and WT mice were used for all experiments. Studies were performed during the day so that the 12:12-h light-dark cycle would not be disturbed.

Only homozygous Fabp-PG mice (Tg/Tg) were used and were confirmed by semiquantitative cycle PCR as described previously (12). As reported earlier (12), the Fabp-PG mice were positive for 0.5–2.0 nM progastrin in the plasma while the FVB/N WT mice were negative for detectable levels of hPG. Circulating levels of amidated gastrins (G17) were similar in Fabp-PG and WT mice (~30 pM).

*Treatment of Mice with NEMO Peptide and Progastrin*—Peptides corresponding to the NEMO-binding domain (NBD) of IKKα or IKKβ specifically inhibit the induction of NFκB activation without inhibiting basal NFκB activity (22). Therefore, to understand the role of induced activation of NFκB in mediating proliferative/antiapoptotic effects of progastrin in Fabp-PG mice, we treated mice with either wtNBD (NEMO peptide) or a control peptide (Imgenex, San Diego, CA) as described (23). Peptides were solubilized in saline and mice-injected intraperitoneal with 1.25 mg per kg body weight, once daily for 4 days. The last injection was given 2 h before killing. For progastrin injections, animals were randomized into two groups and treated with either saline or progastrin (1 nM, 2× day).

*Isolation of Colonic Crypt*—Intact colonic crypts were isolated from mice, as previously described (18, 24). Crypts were imaged on an inverted microscope with a 12-bit gray level charge-coupled device camera. Images were taken at ×200 magnification and crypt length measured by a standard microscale etched onto a glass slide using Metamorph image analysis software (Universal Imaging Corp., Brandywine Parkway, PA). A total of ~150 crypts per group were used for length measurements.

*Subcellular Fractionation, Protein Estimation, and Western Blotting*—Total cellular and nuclear protein extracts were prepared from isolated crypts of either proximal or distal colons of WT and Fabp-PG mice as previously described (18, 25, 26). Total crypt cellular or nuclear extracts (30–100 μg of protein/lane) were processed for Western immunoblot analysis as described (18, 26). Antibodies used for Western immunoblot analysis and for immunohistochemistry (described below) were as follows: polyclonal anti: β-catenin, *p*β-catenin-$Thr^{41}$/$Ser^{45}$, *p*β-catenin-$Ser^{45}$, *p*β-catenin-$Ser^{33,37}$/$Thr^{41}$, *p*GSK-3β-$Ser^{9}$, *p*β-catenin-$Ser^{552}$, and cyclin D1 (CST, Danvers, MA); *p*GSK-3α/β ($Tyr^{279}$/$Tyr^{216}$), lamin B (Santa Cruz Biotechnology, Santa Cruz, CA); monoclonal anti-β-catenin (dephospho 8E4 clone, EMD Biosciences, San Diego, CA); monoclonal anti-actin and anti-histone (Chemicon International, Temecula, CA).

*Immunohistochemical (IHC) Staining of the Colonic Crypts for PCNA and β-Catenin*—IHC for PCNA and phospho β-catenin (*p*β-$cat^{41}$/$^{45}$) (primarily recognizing β-catenin phosphorylated at $Ser^{45}$) was performed on 5-μm-thick frozen sections from proximal and distal colons of Fabp-PG mice and their WT littermates utilizing the horseradish peroxidase-labeled polymer conjugated to secondary antibody using Envision+System-HRP (DAB; DakoCytomation, Carpinteria, CA) with microwave accentuation as described (18, 25, 26). Antibody controls included either omission of the primary antibody or detection of endogenous IgG staining with goat anti-mouse or anti-rabbit IgG (Calbiochem, San Diego, CA). The visualization was carried out either via light or fluorescent microscopy.

*Goblet Cell Staining of Sections from WT and Fabp-PG Mice*—The colons were processed for preparing paraffin-embedded sections from distal and proximal colons of WT and Fabp-PG mice by our published methods (12). In experiments where the mice were treated with either the specific NEMO peptide or the control (mutant) peptide (as described above), the proximal and distal colons from the Fabp-PG mice were processed for preparing frozen sections by our

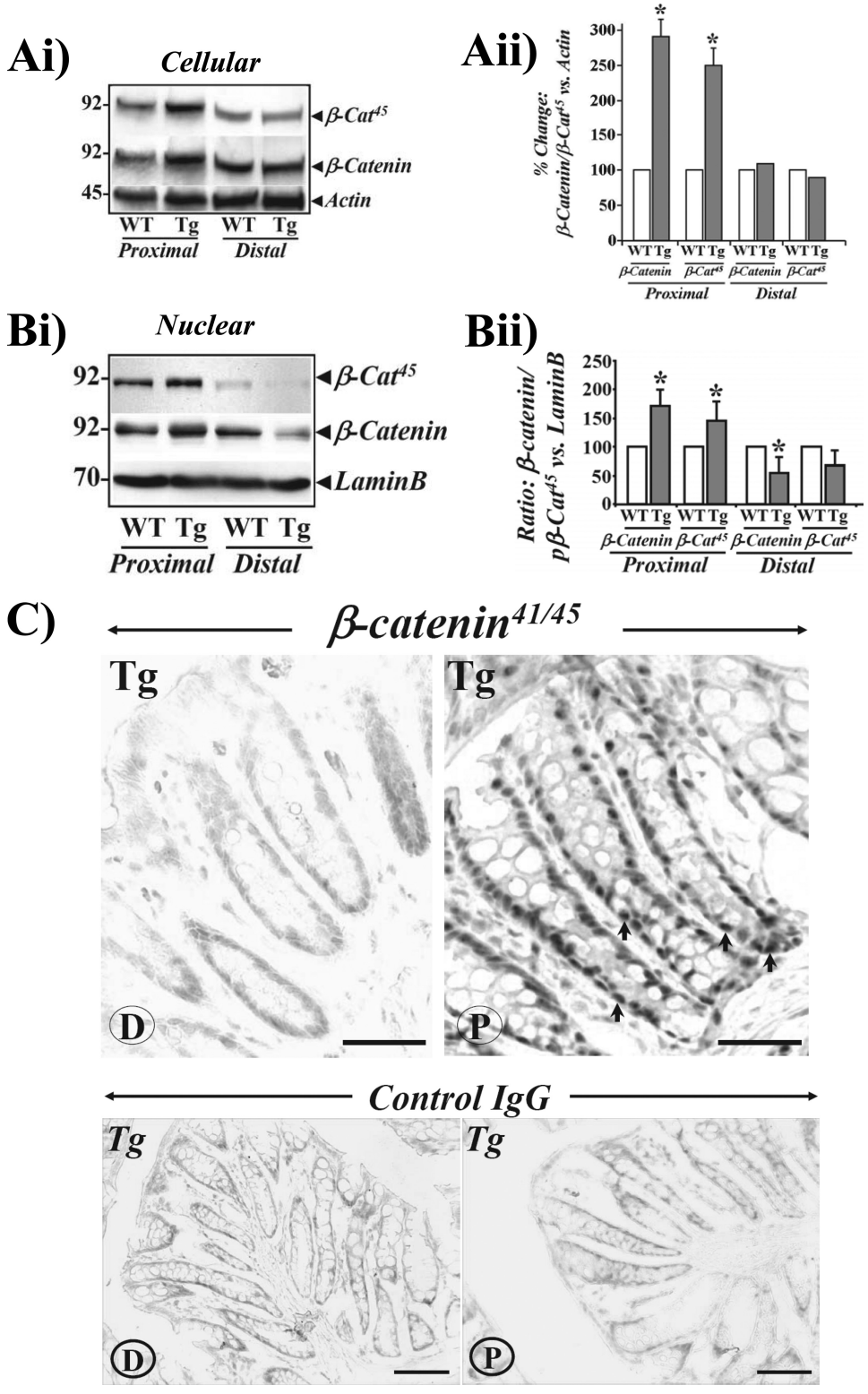


FIGURE 1. **Relative levels of phosphorylated and total β-catenin in proximal (*P*) and distal (*D*) colons of Fabp-PG (Tg) and WT mice.** Western blots showing relative levels of phosphorylated and total β-catenin in cellular (*Ai*) and nuclear (*Bi*) extracts prepared from proximal and distal colonic crypts of WT and Tg mice are shown. *Aii* and *Bii*, Western blots of cellular and nuclear extracts from isolated crypts were densitometrically analyzed, and the ratio of total β-catenin and β-cat$^{45}$ to β-actin/lamin B for WT samples was arbitrarily assigned a 100% value. The percent change in ratios for Fabp-PG *versus* WT samples is shown as *bar graphs*. Data in each bar graph represent mean ± S.E. of three blots from three mice. *, $p < 0.05$ *versus* WT values. *C*, IHC of frozen sections with antibody for β-catenin phosphorylated at Thr$^{41}$/Ser$^{45}$ in distal (*D*) and proximal (*P*) colons of Fabp-PG mice (*upper panel*). *Arrows* indicate phosphorylated β-cat$^{45}$ in the nuclei of colonic crypts ($n = 3$; bar = 50 μm). The *lower panel* represents the IHC with control IgG.

published procedures (18). Both the paraffin-embedded sections and the frozen (fixed) sections were stained with 1% Alcian Blue dissolved in 3% acetic acid followed by counterstaining with 0.1% Nuclear Fast Red using standard histological methods (21).

## RESULTS

We recently reported a significant increase in the length of proximal (P) colonic crypts of Fabp-PG *versus* WT littermates, while the length of colonic crypts from distal (D) half of the colon was similar in the two groups; NFκB activation was critical for measuring proliferation and anti-apoptotic effects of progastrin (18). As a continuation of the studies, the possible contribution of the Wnt/β-catenin pathway was examined in the observed biological effects of progastrin. Casein kinase Iε (CKIε) and GSK-3β phosphorylate β-catenin at Ser$^{45}$ (pβ-cat$^{45}$) and Thr$^{41}$/Ser$^{37,33}$ (pβ-cat$^{33,37,41}$) residues, thereby facilitating its ubiquitination and proteasomal degradation (20). Total crypt extracts, probed by Western blotting, demonstrated significant increases in levels of pβ-cat$^{45}$ in proximal colons of Fabp-PG (Tg) *versus* WT mice (Fig. 1, *Ai*). Results from distal colons of Tg *versus* WT mice were only modestly different (Fig. 1, *Ai*). Ser$^{45}$ phosphorylation, normalized to total β-catenin levels, demonstrated only subtle enhancement in Ser$^{45}$ phosphorylation, suggesting that increased levels of pβ-cat$^{45}$ in proximal colons of Tg mice may be due to a proportional increase in β-catenin abundance in Tg *versus* WT mice. In Fig. 1, *Aii*, relative changes in levels of β-catenin and pβ-cat$^{45}$, normalized to β-actin, are presented as bar graphs from three separate mouse samples. A significant increase in nuclear accumulation of β-catenin and pβ-cat$^{45}$ was similarly recorded in proximal colons of Fabp-PG *versus* WT mice (Fig. 1, *Bi*). While nuclear accumulation was detectable in distal colons of Tg and WT mice, the levels were

much lower in Tg mice (Fig. 1, *Bi*). Data from three separate mouse samples are presented as bar graphs in Fig. 1, *Bii*, as a ratio of lamin B in the samples.

To confirm the dramatic difference in intracellular distribution of β-catenin in proximal *versus* distal colons of Fabp-PG mice, immunohistochemistry of frozen sections was performed. Distal colon sections, stained with anti-phospho-β-cat$^{41/45}$ exhibited relatively weak and barely detectable staining at the base and along the crypt axis (Fig. 1*C*). However, proximal sections exhibited significant increase in cytoplasmic and nuclear staining (Fig. 1*C*), which correlated with biochemical studies (Fig. 1, *A* and *B*). The immunohistochemical results with antibody against total β-catenin levels were identical to that presented in Fig. 1*C* (data not shown.) Sections stained with control IgG (Fig. 1*C*, *lower panels*) did not exhibit specific staining.

We have recently shown that proliferative and antiapoptotic effects of progastrin on proximal but not distal colonic crypts of Fabp-PG mice were attenuated to wild-type levels on treatment with NEMO peptide (18). Recent studies with human embryonic kidney cells *in vitro* suggested that β-catenin signals downstream to the IKKβ/NFκB pathway in response to progastrin (27). To investigate if a similar paradigm holds true *in vivo*, Fabp-PG mice were treated with either NEMO peptide, an inhibitor of IKKα/β, or control (mutant) peptide as described under "Experimental Procedures." We recently reported that treatment of Fabp-PG mice with the specific NEMO peptide had no affect on activation of ERKs and p38, but significantly reduced activation of IKKα/β and NFκBp65; thus confirming the specificity of the effects of the NEMO peptide on the activation of the IKKα/β/NFκBp65 signaling pathway (18). Relative levels of β-catenin were quite high in proximal colonic crypts of mice treated with control peptide (Fig. 2, *Ai*), similar to that measured in non-treated Fabp-PG mice (Fig. 1*A*). Treatment with NEMO peptide, however, blocked the increase in cellular β-catenin in proximal colons (Fig. 2*Ai*). Neither control nor NEMO peptide had any affect on cellular levels of β-catenin in distal colons; bar graphs show relative changes in levels of β-catenin *versus* actin from four mouse samples (Fig. 2, *Ai*). Because activation of the Wnt pathway leads to accumulation of unphosphorylated β-catenin, we next measured the effect of NEMO peptide treatment on relative levels of dephosphorylated and total β-catenin in cytosol and nuclear extracts of proximal colonic crypts from Fabp-PG mice. While relative levels of total β-catenin remained elevated in cytosolic and nuclear extracts of proximal crypts from control peptide-treated mice, NEMO peptide treatment significantly reduced the levels of total β-catenin in cytosolic and nuclear extracts of proximal crypts from Fabp-PG mice (Fig. 2, *Aii*). Cytosolic levels of dephosphorylated β-catenin in control peptide-treated mice were low and did not change in response to NEMO treatment (Fig. 2, *Aii*). Nuclear translocation of dephosphorylated β-catenin, however, decreased significantly in proximal crypts of mice treated with NEMO *versus* that measured in controls (Fig. 2, *Aii*). Bar graphs in Fig. 2, *Aii* show relative changes in levels of total and dephosphorylated β-catenin *versus* actin/histone levels ($n = 4$). These findings provide further evidence that β-catenin activation in proximal colonic crypts may be downstream to activation of IKKα,β/NFκB in Fabp-PG mice.

β-Catenin undergoes constitutive and regulatory phosphorylation at Ser/Thr residues, which affect its stability and subcellular distribution. We next examined the effect of NEMO peptide treatment on moiety-specific phosphorylation of β-catenin in colonic crypts. Data from the cytosol and nuclei of proximal colons from NEMO- and control peptide-treated mice are shown in Fig. 2, *Bi* and *Bii*, respectively. CKIε and GSK-3β facilitate N-terminal phosphorylation of β-catenin at Ser$^{45}$ and Ser$^{33,37}$/Thr$^{41}$ residues, respectively, while kinases such as Akt and cAMP-dependent kinase phosphorylate β-catenin at Ser$^{552}$ (*p*β-cat$^{552}$), which positively regulates transcriptional activity of β-catenin (27, 28). Relative levels of *p*β-cat$^{45}$ and *p*β-cat$^{552}$ were significantly elevated in the cytosol of proximal crypts of control *versus* NEMO peptide-treated mice (Fig. 2, *Bi*), similar to the profile recorded for total β-catenin (see Fig. 2*A*). Cytosolic *p*β-Cat$^{33,37,41}$ levels however exhibited a subtle decrease in the control peptide-treated crypts (Fig. 2, *Bi*). In response to the NEMO peptide, both *p*β-cat$^{45}$ and *p*β-cat$^{552}$ exhibited a significant decrease in relative abundance (Fig. 2, *Bi*), similar to that recorded for total β-catenin (see Fig. 2*A*). *p*β-Cat$^{33,37,41}$, on the other hand, increased significantly after NEMO treatment, suggesting that NEMO may be facilitating activation of kinases such as GSK-3β, thereby promoting phosphorylation of β-catenin at serine 33 and 37 residues in P colonic crypts. Bar graphs in Fig. 2, *Bi* show relative levels of various β-catenin species in relation to actin ($n = 4$).

To determine whether decreases in cellular levels of the phosphorylated β-catenin species in response to the NEMO peptide affected their nuclear import, we next probed crypt nuclear extracts with antibodies for *p*β-cat$^{45}$, *p*β-cat$^{552}$, and *p*β-cat$^{33,37,41}$. Relative levels of nuclear *p*β-cat$^{45}$ and *p*β-cat$^{552}$ were significantly elevated in nuclear extracts of control peptide-treated mice (Fig. 2, *Bii*), similar to levels observed in non-treated Fabp-PG mice (data not shown). *p*β-Cat$^{33,37}$ was also detected in nuclear extracts of proximal crypts from control peptide-treated Fabp-PG mice. In response to NEMO peptide treatment, however, nuclear levels of all three species of β-catenin were significantly decreased (Fig. 2, *Bii*), which may reflect a proportionate decrease in cellular levels of these proteins. Bar graphs in Fig. 2, *Bii* show relative levels of various β-catenin species in the nuclear extracts, normalized to histone ($n = 4$).

Cyclin D1 levels were measured in proximal colonic crypts, as a functional readout of β-catenin activation. Relative levels of cytosolic and nuclear cyclin D1 in proximal crypts were elevated in control peptide-treated mice (Fig. 2*C*). In NEMO peptide-treated mice, a significant decrease in relative levels of cytosolic and nuclear cyclin D1 were measured (Fig. 2*C*), which corroborated our previous findings of attenuation of proliferative effects of progastrin on proximal crypts of NEMO-treated Fabp-PG mice (18). Bar graphs in Fig. 2*C* show relative levels of cyclin D1, normalized to actin/histone levels ($n = 3$).

To explore the possibility that elevated levels of cellular *p*β-cat$^{33,37,41}$ in crypts of NEMO peptide-treated mice (Fig. 2*B*) may be due to a corresponding functional change in GSK-3β, we measured the Ser and Tyr phosphorylation status of

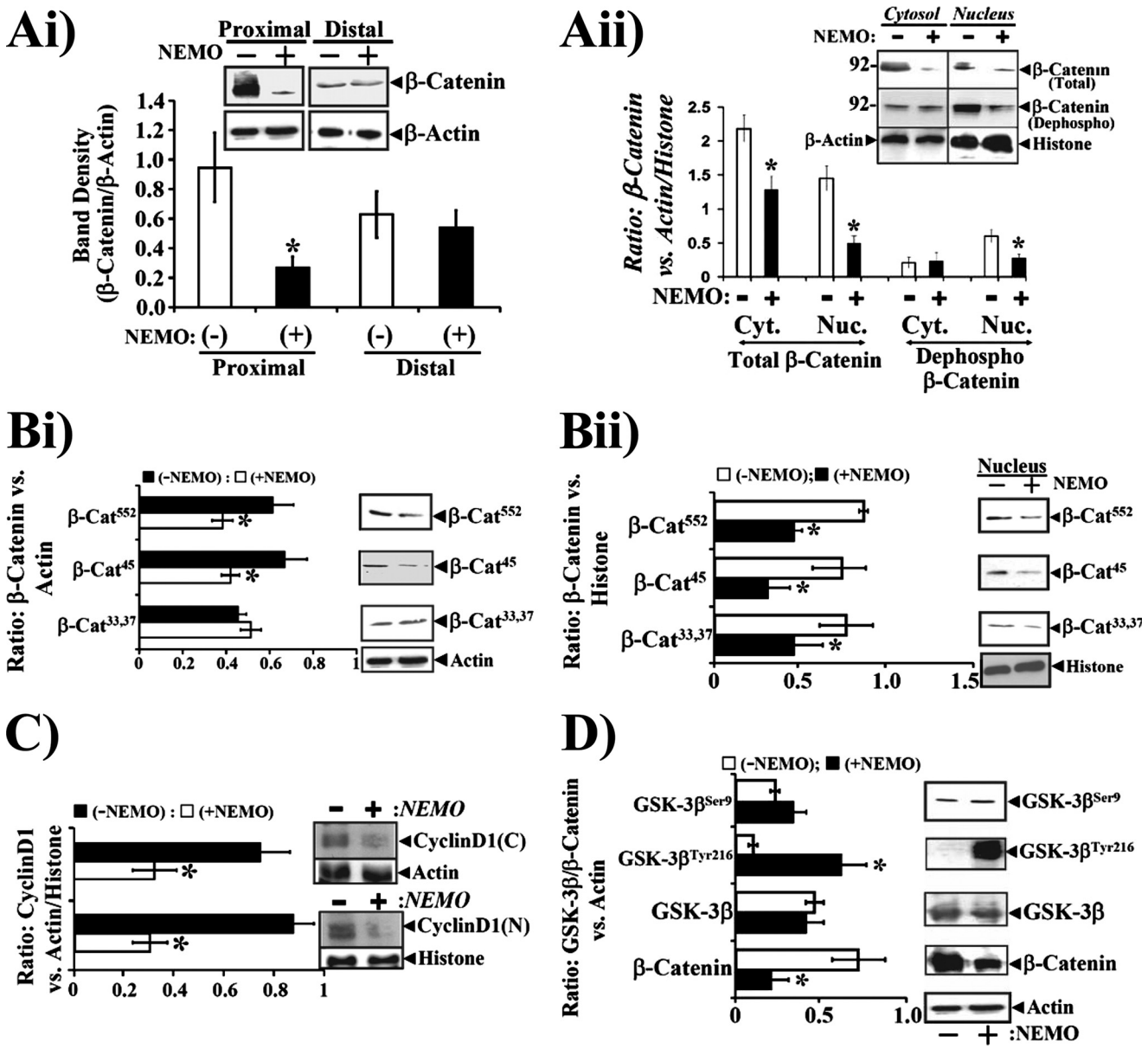


FIGURE 2. **Effect of NEMO peptide on the cytosolic and nuclear levels of total and phosphorylated β-catenin and GSK-3β in relation to cellular/nuclear levels of cyclin D1 in proximal colonic crypts.** Mice were divided into two groups and injected once a day for 4 days with either control (−) or NEMO peptide (+) (see "Experimental Procedures"). 2 h after the last injection, colonic crypts were isolated and fractionated into cytosolic and nuclear extracts. Data obtained from proximal (*A–D*) and distal (*Ai*) colonic crypts of Fabp-PG mice are presented. *Ai–Bii*, representative Western blots for total β-catenin (*Ai*), total and dephospho-β-catenin in cytosol (*Cyt.*), and nucleus (*Nuc.*) (*Aii*); β-Catenin phosphorylated at serine 552, 45, and 33/37/41, respectively, in cytosol (*Bi*) and nucleus (*Bii*) from control (−) *versus* NEMO peptide (+)-treated samples are shown from one of four mice per group. The data in the Western blots of the cellular extracts were densitometrically analyzed from all mouse samples, and the ratios of β-catenin to β-actin or histone were arbitrarily assigned a 100% value. The percent change in ratios for NEMO peptide *versus* control peptide values is shown as *bar graphs*. Data in each bar graph represent mean ± S.E. of four blots from four mice. *C*, effect of NEMO peptide treatment on cyclin D1. Cytosolic (*C*) and nuclear (*N*) crypt extracts prepared from control (−) *versus* NEMO peptide (+)-treated samples were analyzed by blotting with antibody against cyclin D1 (*right panel*). β-Actin and histone were used as loading controls. *Left panel* represents percent change in ratios for NEMO peptide *versus* control peptide shown as *bar graphs* ($n = 3$). *D*, effect of NEMO peptide treatment on GSK-3β in relation to total β-catenin. Western blots showing relative levels of phosphorylated and total GSK-3β along with β-catenin in control (−) and NEMO peptide (+)-treated proximal colonic crypt samples from Fabp-PG mice. Triton X-100-solubilized total crypt extracts were analyzed by blotting with antibodies detecting $Ser^9$-phosphorylated (*GSK-3β-Ser*$^9$) or $Tyr^{216}$-phosphorylated GSK-3β (*GSK-3β-Tyr*$^{216}$), total GSK-3β, and β-catenin. *Left panel* represents the percent change in ratios for NEMO peptide *versus* control peptide shown as *bar graphs* ($n = 3$). β-Catenin levels in proximal and distal colons of control and NEMO-treated WT mice were similar to that in distal colons of Fabp-PG mice (*2Ai*) (data not shown). We previously reported that relative levels of activated IKKαβ/NFκB in control peptide and NEMO peptide-treated WT mice were similar to that measured in distal crypts of Fabp-PG mice (18), because IKKαβ/NFκB are not activated in the distal colons of Fabp-PG mice and remain similar to that in the proximal and distal colons of non-stimulated WT mice.

GSK-3β in proximal crypts of control and NEMO-treated mice. GSK-3β is regulated by multiple mechanisms (28, 29). The kinase is active in the resting cell while it may either be inhibited when it undergoes phosphorylation at $Ser^9$ or activated through phosphorylation at $Tyr^{216}$ in response to a stimulus (30). Relative levels of GSK-3β-$Ser^9$ increased only slightly in NEMO peptide-treated *versus* control samples (Fig. 2*D*). Relative levels of GSK-3β-$Tyr^{216}$, however, increased dramatically by several-fold in NEMO-treated samples compared with control samples, suggesting a significant activation of GSK-3β in response

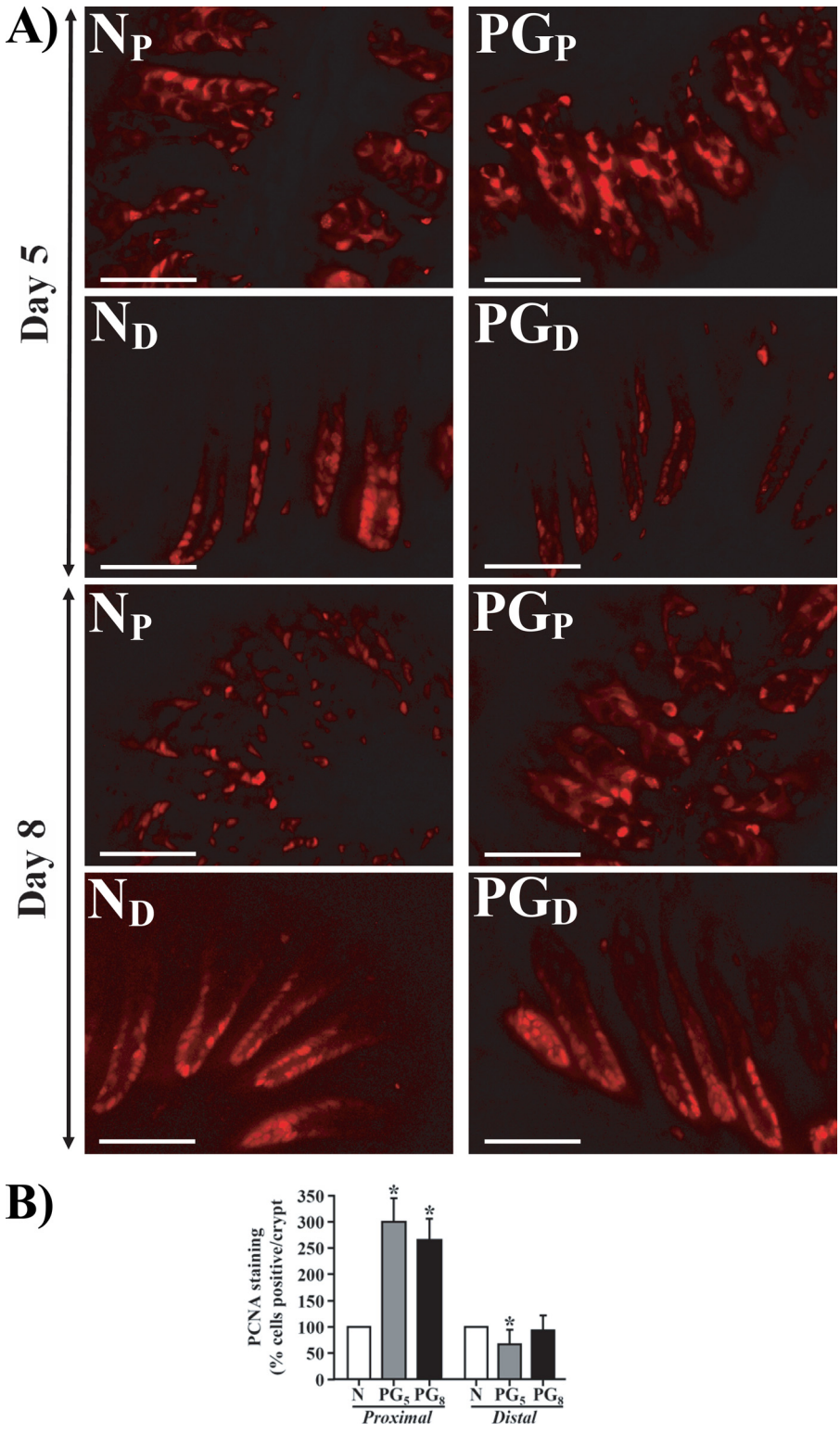


FIGURE 3. **Crypt hyperplasia as measured by PCNA staining.** *A*, immunofluorescent labeling of PCNA as a marker of proliferation in frozen sections prepared from saline-treated control proximal ($N_P$) or distal ($N_D$) colons or 5 and 8 days progastrin-treated proximal ($PG_P$) and distal ($PG_D$) colons. *B*, representative bar graph showing the percent of cells/crypt positive by nuclear staining for PCNA. *Bar*, 75 μm ($n = 3$).

to NEMO treatment. Relative levels of total GSK-3β remained similar in control and NEMO-treated samples (Fig. 2*D*). Phosphorylation of GSK-3β at $Tyr^{216}$ activates GSK-3β (30, 31) and may be causally linked to increases in pβ-cat[33,37,41] in NEMO-treated samples (Fig. 2*B*). Phosphorylation at $Ser^{33,37}$ residues in β-catenin leads to its degradation via the ubiquitin/proteasomal pathway (32). When we reprobed the same membrane with anti-β-catenin antibody, we measured a dramatic decrease in total β-catenin in NEMO-treated samples (Fig. 2*D*), similar to that recorded earlier (Fig. 2*A*). Bar graphs in Fig. 2*D* show relative levels of GSK-3β and β-catenin normalized to actin ($n = 3$). Because activation of NFκB is critical for measuring proliferative and anti-apoptotic effects of progastrin on proximal crypts of Fabp-PG mice (18), it remains to be determined if β-catenin activation, downstream to IKKα,β/NFκB activation (as measured in the current studies), plays an equally important role in the hyperplasia of proximal colonic crypts in response to progastrin.

*Proliferation of Colonic Crypt Cells in WT FVB/N Mice Treated with Progastrin*—Fabp-PG mice represent a chronic model of progastrin stimulation via autocrine/paracrine routes. Differences in the interaction of endogenous progastrin with its high affinity receptor, AnnexinII (33), in proximal *versus* distal crypts may have contributed to significant differences in the biological response of proximal *versus* distal crypts to chronically elevated progastrin levels in Fabp-PG mice (18). To determine if these differences are an artifact of chronic stimulation, we investigated the effects of acutely stimulating WT FVB/N mice with progastrin. Mice injected with 1 nM progastrin, twice a day, were positive for ~150–300 pg of progastrin/ml serum (data not shown). Tissue sections (frozen) were prepared from proximal and distal colons of mice, treated for 5 or 8 days with progastrin and stained for PCNA by immunofluorescence, as a marker of proliferation. Representative sections from proximal and distal colons of saline-treated (N) and progastrin-treated mice are shown in Fig. 3*A*. In normally proliferating proximal and distal crypts, only cells at the base, exhibited nuclear staining. In progastrin-treated proximal colons, intense nuclear immunoreactivity extending throughout the longitudinal crypt axis was observed in samples from both days 5 and 8 (Fig. 3*A*). PCNA

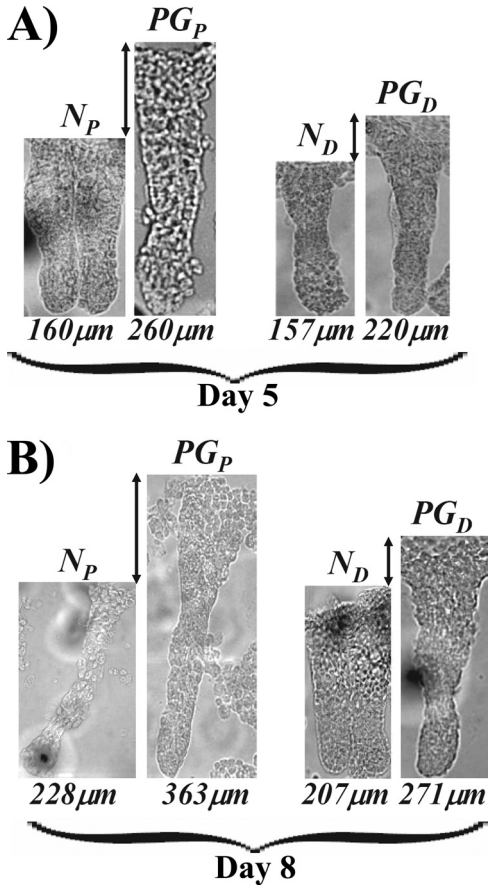


FIGURE 4. **Measurement of crypt lengths in control and progastrin-treated proximal and distal colonic crypts.** Representative images of the intact proximal and distal colonic crypts isolated from saline-treated or progastrin (*PG*)-treated FVB/N mice at 5 and 8 days, respectively ($n = 10$ mice per group). The lengths, shown *under* each crypt, were measured with a standard microscale etched onto a glass slide using Metamorph image analysis software. A total of ~150 crypts per group were used for length measurements.

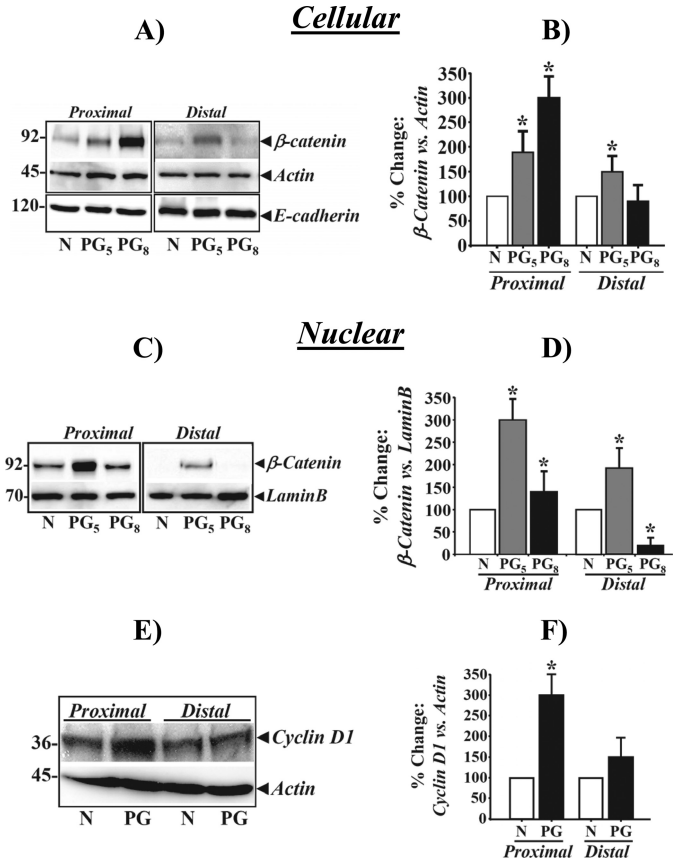


FIGURE 5. **Effect of progastrin treatment on relative levels of β-catenin and E-cadherin in relation to cellular levels of cyclin D1 in colonic crypts.** Representative Western blots showing relative levels of cellular β-catenin and E-cadherin (*A*) and nuclear β-catenin (*C*), with respect to β-actin (*A*) and lamin B (*C*), in proximal and distal colonic crypts of saline-treated (*N*) or 5 and 8 days progastrin (*PG*)-treated FVB/N mice. *B* and *D* represent the ratio of percent changes in β-catenin *versus* β-actin (*B*) and lamin B (*D*), shown as mean ± S.E. of three blots from three mice ($n = 3$). *E*, relative levels of cyclin D1 in control (saline-injected) (*N*) and 5 days post-progastrin-injected crypt cellular extracts from proximal and distal colons, measured via Western blotting. *F*, ratio of percent changes in cyclin D1 *versus* β-actin shown as mean ± S.E. of three blots from three mice ($n = 3$).

staining in distal colons, however, either declined (at day 5) or failed to exhibit significant changes (at day 8) in response to progastrin treatment (Fig. 3*A*). Bar graphs in Fig. 3*B* represent % cells positive for nuclear staining for PCNA/crypt ($n = 15$ sections/miceX3).

The length of isolated crypts was also analyzed (Fig. 4). Crypts isolated from proximal colons of progastrin-treated mice increased significantly ($p < 0.05$) in length by ~40% at days 5 and 8, respectively (Fig. 4, *A* and *B*). The length of the colonic crypts isolated from the distal colons on the other hand exhibited only subtle changes in response to progastrin treatment (Fig. 4, *A* and *B*). Thus, proliferative effects of progastrin were significantly more pronounced on proximal *versus* distal colonic crypts, similar to data obtained with the chronic model of stimulation (Fabp-PG mice) (18). The latter results provide further evidence that differences in the interaction of progastrin with AnnexinII in proximal *versus* distal colonic crypts, as previously reported (18), may reflect an inherent difference in the biology of proximal *versus* distal crypts (as discussed in Ref. 18) and is likely the underlying reason for the observed differences in the response of proximal *versus* distal colonic crypts to progastrin. This possibility needs to be confirmed in future studies with mice down-regulated for AnnexinII expression.

*Cellular and Nuclear Changes in β-Catenin Levels in Response to Progastrin Injections in Proximal and Distal Colonic Crypts of WT FVB/N Mice*—A significant increase in relative levels of cellular and nuclear β-catenin at days 5 and 8 was measured in proximal crypts of progastrin stimulated *versus* control mice (Fig. 5, *A* and *C*). In distal crypts, however, only day 5 animals showed any significant alteration in cellular and nuclear levels of β-catenin; day 8 crypt extracts were barely positive for β-catenin (Fig. 5, *A* and *C*). β-Catenin levels were generally lower in proximal *versus* distal crypts of untreated mice (Fig. 5), once again suggesting inherent differences in the biology of distal *versus* proximal crypts. Bar graphs in Fig. 5, *B* and *D* show % change in ratios of cellular and nuclear β-catenin *versus* actin/lamin B in proximal and distal colons at days 5 and 8 post-treatment. As a functional readout of β-catenin activation, relative levels of cyclin D1 were measured. Representative Western blots for day 5 samples demonstrating cyclin D1 levels are shown in Fig. 5*E*. Relative levels of cyclin D1 increased sig-

nificantly in proximal but not distal crypts of progastrin-treated *versus* control mice. Bar graphs in Fig. 5*F* show % changes in the ratio of cyclin D1 *versus* actin in proximal and distal colons at day 5 of treatment. Thus, progastrin treatment of WT mice induced changes in intracellular signaling in proximal colonic crypts similar to that recorded in Fabp-PG mice, which confirmed that differences measured in the response of proximal *versus* distal colonic crypts likely represent an inherent difference in the biology of the crypts in the two parts of the colon (as recently discussed, Ref. 18).

*Goblet Cell Hyperplasia in Proximal versus Distal Colons of Fabp-PG Mice*—Colonic goblet cell hyperplasia has been reported in hGAS mice, which secrete 100–1000 nM progastrin from the liver (9). Because Fabp-PG mice express significantly lower levels of progastrin (<1.0–5 nM) from the intestinal epithelium (12), we examined the colonic crypts from proximal and distal colons for the possible presence of goblet cell hyperplasia (as measured in the hGAS mice). As shown in Fig. 6, *Ai* (*left panel*), a significant difference was not recorded in the pattern of goblet cell staining in the proximal and distal colonic crypts of WT mice. In Fabp-PG (Tg/Tg) mice, however, proximal colons exhibited a significant increase in goblet cell hyperplasia while goblet cell hyperplasia was less pronounced in distal colons of the Fabp-PG mice (Fig. 6, *Ai*, *right panel*). Interestingly, the majority of the goblet cells in proximal colons were concentrated in the bottom two-thirds of the crypt, while the upper two-thirds of the distal crypts stained positive with Alcian Blue (Fig. 6, *Ai*). Bar graphs in Fig. 6, *Aii* represent the percent of goblet cells/crypt in proximal *versus* distal colons of WT and Fabp-PG mice. Data in Fig. 6, *Ai* confirm the significant difference in the length of the colonic crypts in distal *versus* proximal colons of Fabp-PG mice, as reported previously (18). The height of the proximal and distal colonic crypts in WT littermates was similar to that in the distal colons of Fabp-PG mice (Fig. 6, *Ai*), as previously reported (18).

To investigate the possible involvement of the IKKα,β/NFκB and β-catenin pathways in regulating goblet cell hyperplasia, frozen sections prepared from proximal and distal colons of Fabp-PG mice treated with either control (mutant) peptide or NEMO peptide were stained with Alcian Blue to localize the goblet cells. NEMO peptide treatment of Fabp-PG mice resulted in a significant loss in the percentage of goblet cells/crypt of proximal colons, but not distal colons (Fig. 6, *Bi* and *Bii*), suggesting that IKKα,β/NFκB and/or β-catenin may be involved in regulating goblet cell hyperplasia in proximal colons of Fabp-PG mice. As expected, because distal colons are not responsive to hyperproliferative effects of PG, NEMO treatment of Fabp-PG mice did not result in any significant change in the pattern of goblet cell staining in the distal colons of Fabp-PG mice (Fig. 6, *Bi* and *Bii*).

## DISCUSSION

In the current studies, we report for the first time a significant up-regulation and nuclear translocation of both total and dephosphorylated β-catenin along with $p\beta\text{-cat}^{45}$ in proximal colonic crypts of Fabp-PG mice compared with that in the proximal crypts of WT littermates; significant differences were not measured in distal colons. The up-regulation of β-catenin levels was similarly reported in response to progastrin and gastrin peptides in cancer cell lines, *in vitro* (34, 35). We had previously reported a significant difference in the activation of IKKβ/NFκB (downstream of activation of ERKs/MAPKp38) in proximal *versus* distal colons of Fabp-PG mice (18). Our findings suggested that both an increase in proliferation and a decrease in azoxymethane-induced apoptosis (18) may have contributed to the significant increase in proximal colon carcinogenesis reported in Fabp-PG mice (12). It is thus possible that both an increase in NFκB activation (18) and an increase in β-catenin activation (current studies) are required for measuring hyperplasia of proximal colonic crypts in response to progastrin in Fabp-PG mice. Recently, we reported that activation of NFκB in pancreatic cancer cells (*in vitro*) (11) and in proximal colonic crypts (*in vivo*) (18) is critically required for measuring proliferative and anti-apoptotic effects of progastrin. It was therefore important to learn whether β-catenin activation, as measured in the current studies, was perhaps related to the previously reported NFκB activation in response to progastrin.

Mice were treated with NEMO peptide (an inhibitor of IKKα,β/NFκB activation) and components of the Wnt pathway analyzed in proximal and distal colonic crypts. NEMO treatment significantly blocked the increase in relative levels of total β-catenin/dephospho-β-catenin/and $p\beta\text{-cat}^{45}$ and $p\beta\text{-cat}^{552}$ in proximal, but not distal, colonic crypts, suggesting that β-catenin signals downstream to the IKKα,β/NFκB pathway. The decrease in $\beta\text{-cat}^{45}$ or $\beta\text{-cat}^{552}$ may be attributed to an overall decrease in total β-catenin in proximal colonic crypts in response to NEMO. However, increases in the $\beta\text{-cat}^{33,37}$ species in proximal colonic crypts after NEMO treatment suggest that an upstream event such as activation of GSK-3β rather than β-catenin protein level may be more relevant in regulating β-catenin stability in response to NEMO treatment. Given that GSK-3β along with APC play an important role in the regulation of β-catenin turnover, we further explored the possibility that GSK-3β may be involved in NEMO peptide-induced inhibition of β-catenin activation *in vivo*. NEMO peptide treatment led to dramatic increases in $Tyr^{216}$ phosphorylation of GSK-3β in proximal colonic crypts of Fabp-PG mice without significantly altering phosphorylation at $Ser^{9}$. Because phosphorylation of GSK-3β at $Tyr^{216}$ in its catalytic domain leads to its activation (31), it is tempting to speculate that the increases in $p\beta\text{-cat}^{33,37,41}$ observed in NEMO-treated proximal colonic crypts may be catalyzed by activated GSK-3β, leading eventually to degradation of β-catenin. Conversely, our results also suggest that $Tyr^{216}$ phosphorylation of GSK-3β is significantly attenuated in proximal crypts of Fabp-PG mice, resulting in stabilization/nuclear translocation of β-catenin in response to progastrin in Fabp-PG mice. These results represent one of the most significant findings of the current studies, providing a mechanistic link to the previously reported critical requirement for activation of NFκB for measuring growth effects of progastrin on proximal colonic crypts. It remains to be determined if activation of β-catenin, downstream of IKKβ/NFκB, is also critically required for measuring hyperplasia of proximal colonic crypts in response to elevated levels of progastrin.

In previous studies, disruption of β-catenin and E-cadherin complexes at the membrane has been reported in response to

progastrin in some cell lines, resulting in increased availability of cellular β-catenin (36). In a progastrin-secreting human colon cancer cell line (DLD-1), down-regulation of gastrin gene expression (and hence progastrin) restored membrane localization of β-catenin and E-cadherin (36), providing indirect evidence that progastrin-like peptides can increase cytosolic β-catenin. Besides non-amidated gastrins (progastrin and G-gly), amidated gastrins (G17) have also been reported to up-

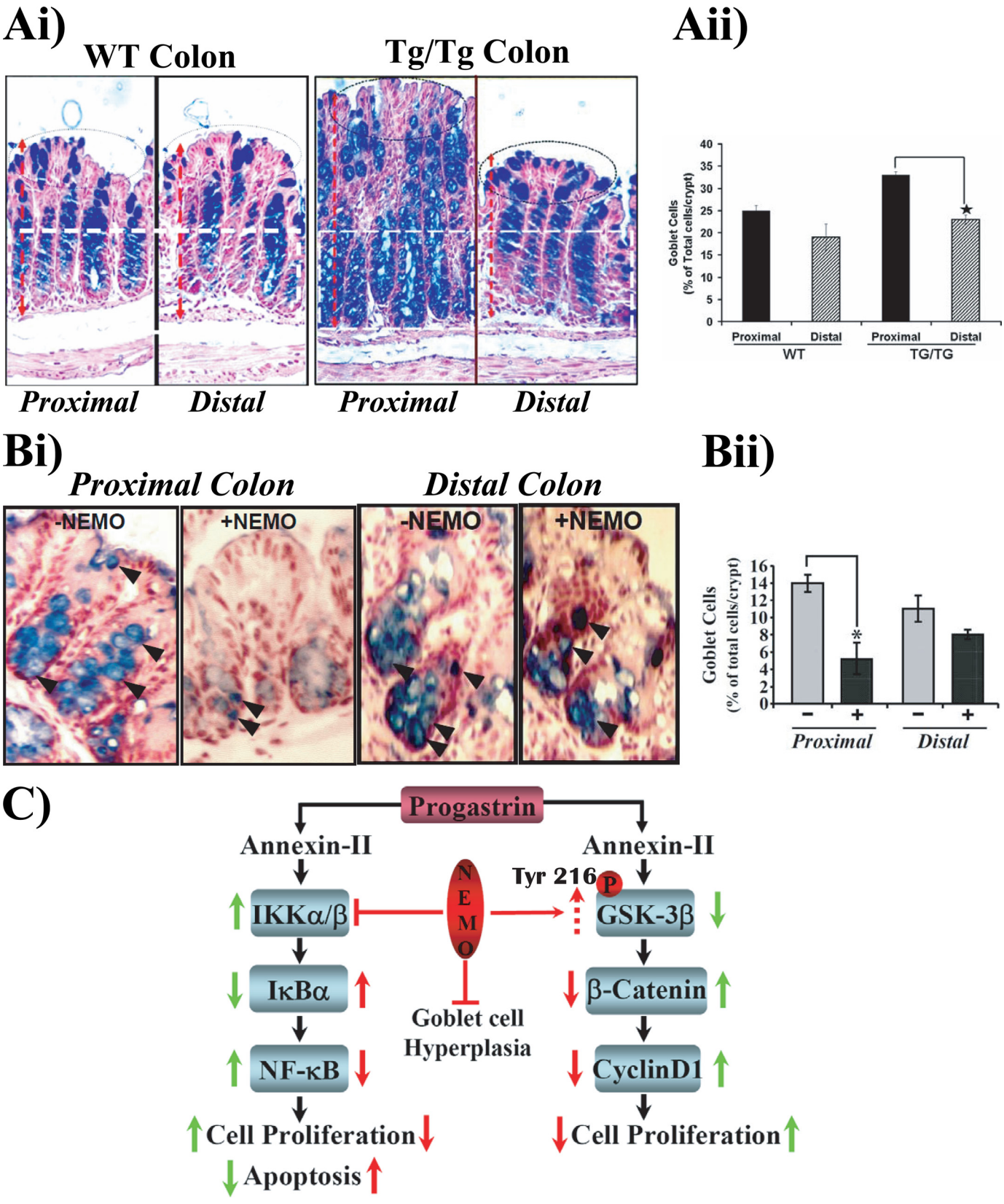

regulate/stabilize β-catenin (37). In a gastric adenocarcinoma cell line, G17 was reported to significantly up-regulate cyclin D1 transcription via both the β-catenin and CREB pathways (38). The results of our current studies suggest that a significant increase in the levels of cellular/nuclear β-catenin in proximal crypts of Fabp-PG mice may be secondary to activated IKKα,β/NFκB and perhaps mediated by the loss of activating phosphorylation of GSK-3β on the $Tyr^{216}$ moiety. Activation of GSK-3β in response to external stimuli is not unprecedented. Utilizing wild type *Salmonella typhimurium* infection, Duan *et al.* (39) reported that bacterial infection stimulated phosphorylation of β-catenin at $Ser^{33,37}$ residues via activated GSK-3β ($Tyr^{216}$) in colonic epithelial cells, leading to degradation of β-catenin and negative regulation of both Wnt and NFκB signaling. Thus multiple pathways mediate an increase in cellular levels of β-catenin, which may be cell- and stimulus-specific.

Cross-talk between the Wnt and IKK/NFκB signaling pathways has been demonstrated by several investigators (40–44). IKKα positively regulates β-catenin-dependent transcriptional activity by increasing cytosolic levels of β-catenin (40, 41). Stabilization of cytosolic β-catenin by IKKα was mediated by inhibiting both canonical and non-canonical degradation pathways of β-catenin (42). Transcriptional regulation of cyclin D1 was blocked by inhibitors of various kinases including IKKα (43), suggesting a positive cross-talk between IKKα/β and β-catenin. The observed increase in cyclin D1 levels in the proximal colons of Fabp-PG mice likely represents the activation of NFκB and/or β-catenin signaling pathways.

In recent studies, lzts2 (leucine zipper tumor suppressor 2), was shown to interact with β-catenin and repress the transactivation of β-catenin by perhaps affecting the subcellular localization of β-catenin (45). Interestingly, it was found that NFκB regulates expression of lzts2 (46), suggesting a complex interaction between the β-catenin/Tcf and NFκB signaling pathways. While NFκB positively regulated the β-catenin/Tcf pathways in human glioblastoma cell lines (47), negative regulation of NFκB by β-catenin has also been reported in some cancer cell lines (48), suggesting that the nature of the cross-talk between NFκB and β-catenin may be cell-specific and perhaps stimulus-specific.

The majority of the studies, however, have demonstrated a positive cross-talk between NFκB and the components of the Wnt pathway (as described above). The presence of positive cross-talk was further substantiated by a recent finding wherein disruption of the murine GSK-3β gene resulted in embryonic lethality caused by severe liver degeneration during mid-gestation due to lack of NFκB (49). Thus, the cross-talk observed in our studies between NFκB and β-catenin is not unprecedented but may be critical for regulating proliferation of proximal colonic crypts in response to progastrin and perhaps other growth factors. Some or all of the growth effects of progastrin may be mediated via β-catenin, downstream of NFκB activation, which remain to be confirmed in future studies.

In a recent study, β-catenin was reported to regulate differentiation of respiratory epithelial cells *in vivo* (50). Activation of β-catenin in respiratory epithelial cells of the developing lung resulted in inhibiting the expression of Foxa2 and caused goblet cell hyperplasia associated with increased staining for specific mucins (50). Both wild type and activated (mutant) β-catenin negatively regulated the expression of the Foxa2 promoter *in vitro* (50). Interestingly, mice overexpressing activated mutant β-catenin in respiratory epithelial cells developed pulmonary tumors in adult mice, and the lung epithelium demonstrated goblet cell hyperplasia (50). In our studies with Fabp-PG mice, which are chronically stimulated with progastrin since birth, the observation of goblet cell hyperplasia in proximal colonic crypts may represent sustained activation of β-catenin, downstream of NFκB activation, because NEMO treatment caused a loss of goblet cell hyperplasia (Fig. 6). The Notch pathway controls absorptive *versus* secretory fate decisions in the intestinal epithelium. In the intestine, the direct Notch target gene Hes-1 represses transcription of the bHLH transcription factor Math-1 (51). Intestinal Math-1 expression is required for commitment toward secretory lineages including goblet cells (52). Kruppel-like factor-4 (KLF4) is required for colonic goblet cell development (53), and signaling via the Notch pathway inhibits KLF4 gene expression leading to significant loss of goblet cells (21). The Tcf-4/β-catenin-dependent Wnt pathway has also been shown to regulate KLF4 expression (54). Thus, while we did not measure KLF4 levels in Fabp-PG mice, it is tempting to speculate that chronic PG stimulation may be associated with KLF4 up-regulation leading to goblet cell hyperplasia in proximal colons of Fabp-PG mice.

The results presented in this report thus further confirm the novel paradigm that IKKα,β/NFκB activation is critical for measuring not only growth effects of progastrin on proximal colonic crypt cells (as reported earlier, Ref. 18), but is also critical for measuring activation of the β-catenin pathway, resulting in a significant increase in the relative levels of cyclin D1 in response to acute (Fig. 5, *E* and *F*) and chronic (Fig. 2*C*) stimulation with progastrin. Our studies further suggest the novel possibility that $Tyr^{216}$ phosphorylation of GSK-3β may be directly or indirectly regulated by the IKKα,β/NFκB pathway (as diagrammatically presented in (Fig. 6*C*). A third equally

FIGURE 6. **Goblet cell hyperplasia in P colon of Fabp-PG mice.** *Ai*, proximal and distal colons from WT and Fabp-PG (Tg/Tg) mice showing Alcian Blue staining to localize goblet cells. *Aii*, bar graph showing percent of total goblet cells/crypt from the two parts of the colon. *B*, effect of NEMO peptide treatment on goblet cell hyperplasia. Fabp-PG mice were divided into two groups and injected once a day for 4 days with either control (mutant) NEMO peptide (−) or NEMO peptide (+) as described in the legend to Fig. 2. Sections were stained with Alcian Blue. NEMO peptide treatment significantly blocked goblet cell hyperplasia in proximal but not distal colons (*Bi*). *Bii*, bar graph showing percent of total goblet cells/crypt from the colons of control (−) on NEMO peptide (+)-treated mice. *C*, proposed mechanism for a cross-talk between the IKKβ/NFκB and Wnt/β-catenin pathway. Progastrin interacts with its receptor ANXII, at the plasma membrane (33) and promotes intracellular signaling by up-regulating the IKKα,β/NFκB (18) and Wnt/β-catenin pathways (current studies) in colonic crypts. β-Catenin activation, however, was downstream to IKKα,β/NFκB, because NEMO peptide inhibited β-catenin activation via activating $Tyr^{216}$ phosphorylation of GSK-3β. NEMO peptide also blocked goblet cell hyperplasia implicating the IKKα,β/NFκB and/or Wnt/β-catenin pathways in its regulation. Therefore, the previously reported hyperproliferative and anti-apoptotic effects of progastrin on proximal colonic crypts in Fabp-PG mice (18) may have been mediated by the activation of both IKKαβ/NFκB and β-catenin pathways; the two pathways may be acting either in tandem or β-catenin may mediate all or some of the observed biological effects of progastrin.

intriguing finding was that goblet cell lineage in the colonic crypts of Fabp-PG mice may be regulated via the IKKα,β/NFκB/β-catenin pathways, resulting in colonic crypt hyperplasia and goblet cell hyperplasia. Because goblet cell hyperplasia in lung epithelium is associated with pulmonary tumorigenesis (50), it is tempting to speculate that a significant increase in the risk of colon carcinogenesis in proximal crypts of Fabp-PG mice (as reported earlier, Ref. 12), may be related to the observed goblet cell hyperplasia in the colonic crypts of Fabp-PG mice.

## REFERENCES


1. Rengifo-Cam, W., and Singh, P. (2004) *Curr. Pharm. Des.* **10,** 2345–2358
2. Grabowska, A. M., and Watson, S. A. (2007) *Cancer Lett.* **257,** 1–15
3. Kochman, M. L., DelValle, J., Dickinson, C. J., and Boland, C. R. (1992) *Biochem. Biophys. Res. Commun.* **189,** 1165–1169
4. Van Solinge, W. W., Nielsen, F. C., Friis-Hansen, L., Falkmer, U. G., and Rehfeld, J. F. (1993) *Gastroenterology* **104,** 1099–1107
5. Nemeth, J., Taylor, B., Pauwels, S., Varro, A., and Dockray, G. J. (1993) *Gut* **34,** 90–95
6. Baldwin, G. S., Hollande, F., Yang, Z., Karelina, Y., Paterson, A., Strang, R., Fourmy, D., Neumann, G., and Shulkes, A. (2001) *J. Biol. Chem.* **276,** 7791–7796
7. Seva, C., Dickinson, C. J., and Yamada, T. (1994) *Science* **265,** 410–412
8. Singh, P., Lu, X., Cobb, S., Miller, B. T., Tarasova, N., Varro, A., and Owlia, A. (2003) *Am. J. Physiol. Gastrointest. Liver Physiol.* **284,** G328–G339
9. Wang, T. C., Koh, T. J., Varro, A., Cahill, R. J., Dangler, C. A., Fox, J. G., and Dockray, G. J. (1996) *J. Clin. Invest.* **98,** 1918–1929
10. Wu, H., Owlia, A., and Singh, P. (2003) *Am. J. Physiol. Gastrointest. Liver Physiol.* **285,** G1097–G1110
11. Rengifo-Cam, W., Umar, S., Sarkar, S., and Singh, P. (2007) *Cancer Res.* **67,** 7266–7274
12. Cobb, S., Wood, T., Ceci, J., Varro, A., Velasco, M., and Singh, P. (2004) *Cancer* **100,** 1311–1323
13. Singh, P., Velasco, M., Given, R., Varro, A., and Wang, T. C. (2000) *Gastroenterology* **119,** 162–171
14. Singh, P., Velasco, M., Given, R., Wargovich, M., Varro, A., and Wang, T. C. (2000) *Am. J. Physiol. Gastrointest. Liver Physiol.* **278,** G390–G399
15. Ottewell, P. D., Varro, A., Dockray, G. J., Kirton, C. M., Watson, A. J., Wang, T. C., Dimaline, R., and Pritchard, D. M. (2005) *Am. J. Physiol. Gastrointest. Liver Physiol.* **288,** G541–G549
16. Aly, A., Shulkes, A., and Baldwin, G. S. (2001) *Int. J. Cancer* **94,** 307–313
17. Dockray, G. J., Varro, A., and Dimaline, R. (1996) *Physiol. Rev.* **76,** 767–798
18. Umar, S., Sarkar, S., Cowey, S., and Singh, P. (2008) *Oncogene* **27,** 5599–5611
19. van de Wetering, M., Sancho, E., Verweij, C., de Lau, W., Oving, I., Hurlstone, A., van der Horn, K., Batlle, E., Coudreuse, D., Haramis, A. P., Tion-Pon-Fong, M., Moerer, P., van den Born, M., Soete, G., Pals, S., Eilers, M., Medema, R., and Clevers, H. (2002) *Cell* **111,** 241–250
20. Reya, T., and Clevers, H. (2005) *Nature* **434,** 843–850
21. Zheng, H., Pritchard, D. M., Yang, X., Bennett, E., Liu, G., Liu, C., and Ai, W. (2009) *Am. J. Physiol. Gastrointest. Liver Physiol.* **296,** G490–G498
22. May, M. J., D'Acquisto, F., Madge, L. A., Glöckner, J., Pober, J. S., and Ghosh, S. (2000) *Science* **289,** 1550–1554
23. Dasgupta, S., Jana, M., Zhou, Y., Fung, Y. K., Ghosh, S., and Pahan, K. (2004) *J. Immunol.* **173,** 1344–1354
24. Umar, S., Morris, A. P., Kourouma, F., and Sellin, J. H. (2003) *Cell Prolif.* **36,** 361–375
25. Wang, Y., Xiang, G. S., Kourouma, F., and Umar, S. (2006) *Br. J. Pharmacol.* **148,** 814–824
26. Sellin, J. H., Wang, Y., Singh, P., and Umar, S. (2009) *Exp. Cell Res.* **315,** 97–109
27. Sarkar, S., and Singh, P. (2009) *Novel Cross-regulation and Activation of NFκBp65 and β-Catenin, in Response to Over-expression of Progastrin, in Human Embryonic Kidney Cells (HEK293): Role of Annexin II. 100th AACR Annual Meeting* (No. 5275), April 18–22, Denver, CO
28. Dajani, R., Fraser, E., Roe, S. M., Young, N., Good, V., Dale, T. C., and Pearl, L. H. (2001) *Cell* **105,** 721–732
29. Frame, S., Cohen, P., and Biondi, R. M. (2001) *Mol. Cell* **7,** 1321–1327
30. Doble, B. W., and Woodgett, J. R. (2003) *J. Cell Sci.* **116,** 1175–1186
31. Bhat, R. V., Shanley, J., Correll, M. P., Fieles, W. E., Keith, R. A., Scott, C. W., and Lee, C. M. (2000) *Proc. Natl. Acad. Sci. U.S.A.* **97,** 11074–11079
32. Kitagawa, M., Hatakeyama, S., Shirane, M., Matsumoto, M., Ishida, N., Hattori, K., Nakamichi, I., Kikuchi, A., Nakayama, K., and Nakayama, K. (1999) *EMBO J.* **18,** 2401–2410
33. Singh, P., Wu, H., Clark, C., and Owlia, A. (2007) *Oncogene* **26,** 425–440
34. Pannequin, J., Delaunay, N., Buchert, M., Surrel, F., Bourgaux, J. F., Ryan, J., Boireau, S., Coelho, J., Pélegrin, A., Singh, P., Shulkes, A., Yim, M., Baldwin, G. S., Pignodel, C., Lambeau, G., Jay, P., Joubert, D., and Hollande, F. (2007) *Gastroenterology* **133,** 1554–1568
35. He, H., Shulkes, A., and Baldwin, G. S. (2008) *Biochim. Biophys. Acta* **1783,** 1943–1954
36. Hollande, F., Lee, D. J., Choquet, A., Roche, S., and Baldwin, G. S. (2003) *J. Cell Sci.* **116,** 1187–1197
37. Song, D. H., Kaufman, J. C., Borodyansky, L., Albanese, C., Pestell, R. G., and Wolfe, M. M. (2005) *Br. J. Cancer* **92,** 1581–1587
38. Pradeep, A., Sharma, C., Sathyanarayana, P., Albanese, C., Fleming, J. V., Wang, T. C., Wolfe, M. M., Baker, K. M., Pestell, R. G., and Rana, B. (2004) *Oncogene* **23,** 3689–3699
39. Duan, Y., Liao, A. P., Kuppireddi, S., Ye, Z., Ciancio, M. J., and Sun, J. (2007) *Lab. Invest.* **87,** 613–624
40. Albanese, C., Wu, K., D'Amico, M., Jarrett, C., Joyce, D., Hughes, J., Hulit, J., Sakamaki, T., Fu, M., Ben-Ze'ev, A., Bromberg, J. F., Lamberti, C., Verma, U., Gaynor, R. B., Byers, S. W., and Pestell, R. G. (2003) *Mol. Biol. Cell* **14,** 585–599
41. Lamberti, C., Lin, K. M., Yamamoto, Y., Verma, U., Verma, I. M., Byers, S., and Gaynor, R. B. (2001) *J. Biol. Chem.* **276,** 42276–42286
42. Carayol, N., and Wang, C. Y. (2006) *Cell. Signal.* **18,** 1941–1946
43. Cho, M., Gwak, J., Park, S., Won, J., Kim, D. E., Yea, S. S., Cha, I. J., Kim, T. K., Shin, J. G., and Oh, S. (2005) *FEBS Lett.* **579,** 4213–4218
44. Sun, J., Hobert, M. E., Duan, Y., Rao, A. S., He, T. C., Chang, E. B., and Madara, J. L. (2005) *Am. J. Physiol. Gastrointest. Liver Physiol.* **289,** G129–G137
45. Thyssen, G., Li, T. H., Lehmann, L., Zhuo, M., Sharma, M., and Sun, Z. (2006) *Mol. Cell. Biol.* **26,** 8857–8867
46. Cho, H. H., Joo, H. J., Song, J. S., Bae, Y. C., and Jung, J. S. (2008) *Biochim. Biophys. Acta* **1783,** 419–428
47. Cho, H. H., Song, J. S., Yu, J. M., Yu, S. S., Choi, S. J., Kim, D. H., and Jung, J. S. (2008) *FEBS Lett.* **582,** 616–622
48. Deng, J., Miller, S. A., Wang, H. Y., Xia, W., Wen, Y., Zhou, B. P., Li, Y., Lin, S. Y., and Hung, M. C. (2002) *Cancer Cell* **2,** 323–334
49. Hoeflich, K. P., Luo, J., Rubie, E. A., Tsao, M. S., Jin, O., and Woodgett, J. R. (2000) *Nature* **406,** 86–90
50. Mucenski, M. L., Nation, J. M., Thitoff, A. R., Besnard, V., Xu, Y., Wert, S. E., Harada, N., Taketo, M. M., Stahlman, M. T., and Whitsett, J. A. (2005) *Am. J. Physiol. Lung Cell Mol. Physiol.* **289,** L971–L979
51. Jensen, J., Pedersen, E. E., Galante, P., Hald, J., Heller, R. S., Ishibashi, M., Kageyama, R., Guillemot, F., Serup, P., and Madsen, O. D. (2000) *Nat. Genet.* **24,** 36–44
52. Yang, Q., Bermingham, N. A., Finegold, M. J., and Zoghbi, H. Y. (2001) *Science* **294,** 2155–2158
53. Katz, J. P., Perreault, N., Goldstein, B. G., Lee, C. S., Labosky, P. A., Yang, V. W., and Kaestner, K. H. (2002) *Development* **129,** 2619–2628
54. Flandez, M., Guilmeau, S., Blache, P., and Augenlicht, L. H. (2008) *Exp. Cell Res.* **314,** 3712–3723